OPEN

Enhancing Clinical Diagnosis for Patients With Persistent Pulmonary Abnormalities After COVID-19 Infection

The Potential Benefit of ^{68}Ga-FAPI PET/CT

Anna Sviridenko, MD, Anna Boehm, MD,† Gianpaolo di Santo, MD,* Christian Uprimny, MD,* Bernhard Nilica, MD,* Josef Fritz,‡ Frederik L. Giesel, MD,§|| Uwe Haberkorn, MD,§ Sabina Sahanic, MD,† Clemens Decristoforo, PhD,* Ivan Tancevski, MD,† Gerlig Widmann, MD,¶ Judith Loeffler-Ragg, MD,† and Irene Virgolini, MD**

Abstract: Coronavirus disease 2019 (COVID-19)–related pneumonia challenges clinical practice. We explore the potential diagnostic benefit of PET/CT to establish the underlying inflammatory or fibrotic repair processes in prolonged structural lung abnormalities in COVID-19 patients.

Patients and Methods: Six post COVID-19 patients suspected for pulmonary fibrosis were scheduled for dual-tracer PET/CT with ^{18}F-FDG and ^{68}Ga–fibroblast activation protein inhibitor (FAPI)–46. The uptake of ^{68}Ga-FAPI-46 in the involved lung was compared with a control group of 9 non–COVID-19 patients. Clinical data and PET/CT imaging were collected and analyzed.

Results: PET/CT revealed in all 6 pulmonary impaired patients the reduced glucose avidity on ^{18}F-FDG and clear positivity on ^{68}Ga-FAPI-46 PET/CT in comparison to the control group.

Conclusions: Enhancing fibrotic repair mechanisms, ^{68}Ga-FAPI PET/CT may improve noninvasive clinical diagnostic performance in patients with long-term CT abnormalities after severe COVID-19. Although this study shows promising results, additional studies in larger populations are required to establish a general diagnostic guideline.

Key Words: SARS-CoV-2, ^{68}Ga-FAPI-46 PET/CT, ^{18}F-FDG PET/CT, idiopathic pulmonary fibrosis

(*Clin Nucl Med* 2022;47: 1026–1029)

After a severe course of COVID-19, a pulmonary injury appears to persist in some individuals.[1–3] Whether those prolonged structural lung abnormalities in COVID-19 patients are mainly triggered by underlying inflammatory or fibrotic repair processes has not yet been answered.

Within incidental acute SARS-CoV-2, ^{18}F-FDG PET/CT already proved to discriminate between morphometabolic patterns reflecting the evolutionary phases of inflammatory processes.[4] However, the role of ^{18}F-FDG PET/CT within the diagnostic pathway of long-term pulmonary changes after SARS-CoV-2 infection remains elusive.

The fibroblast activation protein (FAP) expresses on fibroblasts during tissue remodeling, tissue repair, and carcinogenesis.[5,6] Moreover, FAP is selectively induced in activated fibroblasts in a murine model of pulmonary fibrosis.[7,8]

Recently, ^{68}Ga–fibroblast activation protein inhibitor (FAPI) PET/CT could visualize increased tracer uptake in several malignant tumors, such as bronchogenic adenocarcioma but also in fibrotic lesions exemplary in idiopathic pulmonary fibrosis (IPF).[9–13]

PATIENTS AND METHODS

Subjects and Study Design

Between October 2020 and June 2021, 6 patients with a confirmed diagnosis of COVID-19 participated in the prospective CovILD study. The trial protocol was approved by the institutional review board at Innsbruck Medical University (EK Nr: 1103/2020) and was registered at ClinicalTrials.gov (registration number NCT04416100). Signed informed consent was obtained from each patient. The inclusion criteria were (1) post COVID-19 positive cases; (2) patients with persisting exertional dyspnea despite the prolonged high-dose corticosteroids up to 3 months after discharge; (3) at least 3 weeks off corticosteroid therapy before ^{18}F-FDG PET/CT scan; (4) patients underwent thin-section chest CT scans at least twice during the hospitalization and had at least one follow-up CT after discharge with the evidence of persistent lung abnormalities; (5) patients with both ^{18}F-FDG PET/CT and ^{68}Ga-FAPI PET/CT scan after discharge.

Detailed characteristics of the patient's post COVID-19 cohort are shown in Table 1.

One of 6 post COVID-19 patients presented a history of peripheral venous thrombosis. No other manifestation of thrombosis, especially a pulmonary embolism, was noted.

Nine oncological patients with different extrapulmonary tumor entities and no evidence of lung density abnormalities at chest CT underwent ^{68}Ga-FAPI PET/CT and were included as a control group of non–COVID-19 patients.

CT and PET/CT Imaging

All patients had a thin-section chest CT scan performed within the 30 days timespan before the first PET/CT. These high-resolution CT scans were performed on a 1280-slice multidetector CT (SOMATOM

Received for publication May 19, 2022; revision accepted August 23, 2022.

From the Departments of *Nuclear Medicine, †Internal Medicine II, and ‡Radiology, Medical University of Innsbruck, Innsbruck, Austria; §Department of Nuclear Medicine, University Hospital Heidelberg, Heidelberg; ||Department of Nuclear Medicine, University Hospital Düsseldorf, Heinrich-Heine-University, Medical Faculty, Düsseldorf, Germany; and ¶Department of Medical Statistic and Informatics, Medical University of Innsbruck, Innsbruck, Austria.

Conflicts of interest and sources of funding: F.L.G. is an advisor at ABX, SOFIE Biosciences, and Telix Pharmaceutical. F.L.G. and U.H. have a patent application for quinolone-based FAP-targeting agents for imaging and therapy in nuclear medicine and also have shares of a consultancy group for iTheranostics. No conflicts of interest exist for A.B., A.S., S.S., G.S., J.F., C.U., B.N., I.T., G.W., I.V., and J.L.R.

Correspondence to: Anna Sviridenko, MD, Department of Nuclear Medicine, Medical University of Innsbruck, Anichstraße 35, 6020 Innsbruck, Austria. E-mail: anna.sviridenko@tirol-kliniken.at.

ISSN: 0363-9762/22/4712–1026
DOI: 10.1097/RLU.0000000000004437

TABLE 1. Demographics and Clinical Characteristics of Enrolled Post COVID-19 Patients

Patient No.	Sex	Age, y	Time From the COVID Positivity to PET/CT, d	Treatment During Infection	Time From ^{68}Ga-FAPI to ^{18}F-FDG PET/CT, d	Thromboinflammatory Biomarker at Time of ^{68}Ga-FAPI PET/CT vs 1 Year Follow-up
1	F	71	177	Oxygen supply	10	Normal/normal
2	M	57	229	Invasive ventilation	14	Normal/normal
3	M	79	203	Oxygen supply	13	Normal/normal
4	M	70	181	Invasive ventilation	8	Normal/normal
5	M	54	193	Invasive ventilation	14	Increase/increase
6	M	49	147	Invasive ventilation	13	Normal/normal

Defintion Flasch; Siemens Healthineers) with a 128 × 0.6-mm collimation and spiral pitch factor of 1.1.

The PET/CT scans were performed on a dedicated PET/CT system (Discovery DMI; GE Healthcare, Milwaukee, WI) and conducted according the lastly published Declaration of Helsinki.[14] Patients were first scheduled for ^{68}Ga-FAPI PET/CT, which was then followed by an ^{18}F-FDG PET/CT within 14 days.

^{68}Ga-FAPI PET/CT Imaging

^{68}Ga-FAPI-46 was prepared in a procedure similar to that recently described.[15] Before tracer injection, a low-dose CT scan was performed for attenuation correction of the PET emission data. The scan parameters using smart mA dose modulation were as following: 100 kVp, 20–100 mA, noise index 51, 0.5 seconds per tube rotation, slice thickness 3.75 mm, and pitch 0.98. Next, an average dosage of 220 ± 34 MBq (mean ± SD) ^{68}Ga-FAPI-46 was administered intravenously, and a 3-dimensional (3D) dynamic PET scan was performed at tracer injection time. It consisted of 12 × 10 seconds/frame and 36 × 30 seconds/frame acquisitions and was positioned over the lungs. The dynamic scan was followed by static 3D whole-body scans (skull base to upper thighs) with an acquisition time of 2 minutes per bed position, at 30, 60, and 120 minutes postinjection. The PET axial field of view was 20 cm per bed position. The control group only had the 60 minutes postinjection scan.

PET reconstructions were performed using the vendor's block sequential regularized expectation maximization penalized-likelihood (BSREM) such as reconstruction algorithm Q.Clear (GE Healthcare) with a penalization factor ß of 1000.

^{18}F-FDG PET/CT Imaging

For ^{18}F-FDG PET/CT, an acquisition protocol according to the guidelines of the European Association of Nuclear Medicine was applied including a fasting period of at least 6 hours before FDG administration.[16] The median blood glucose level at injection time was 102 mg/dL (range, 115–87 mg/dL). None of our COVID-19 patients had diabetes or insulin treatment or both. The injected dose was 3 MBq/kg, and the uptake time was 60 minutes. First, a low-dose CT was obtained for PET attenuation correction, using the same parameters as described before. Next, a static 3D whole-body PET scan (skull base to upper thighs) with an acquisition time of 2 minutes per bed position was obtained. PET reconstructions were again performed with Q.Clear, with a penalization factor ß of 450.

Image Analysis

First, a visual assessment for elevated trace uptake (higher than mediastinal blood poll) was performed. Then, for semiquantitative analysis, the SUV_{max} and target-to-background ratio (TBR) were calculated. The SUV_{max} values in pulmonary impaired post COVID-19 patient group were obtained by manually drawing the same volumes of interest (VOIs) on the axial PET images in both ^{18}F-FDG and ^{68}Ga-FAPI scans, based on the suspected fibrotic area, as indicated by the high-resolution CT.

The average SUV_{max} of multiple VOIs was obtained for both ^{18}F-FDG and ^{68}Ga-FAPI scans.

The TBR values were calculated by dividing the average SUV_{max} of the fibrotic area by the SUV_{mean} of the blood pool, which was measured by placing a 15-mm diameter spherical VOI in the center of right atrium.

In the pulmonary impaired post COVID-19 patient group, the average SUV_{max} and TBR were calculated for the ^{68}Ga-FAPI scans at 30, 60, and 120 minutes, and for the ^{18}F-FDG scans.

In the control group of non–COVID-19 patients, the SUV_{max} behind the lung parenchyma was obtained by manually drawing multiple VOIs on the axial ^{68}Ga-FAPI PET scan. The average SUV_{max} and TBR were calculated for the ^{68}Ga-FAPI scans at 60 minutes.

The average ^{68}Ga-FAPI SUV_{max} and TBR values at 60 minutes obtained in the pulmonary impaired group were compared with corresponding values in the control group.

In addition, the correlation between the ^{68}Ga-FAPI parameters at 60 minutes and the ^{18}F-FDG equivalents in the pulmonary impaired patient group were analyzed.

The dynamic PET images were used to analyze the ^{68}Ga-FAPI uptake in blood pool and fibrotic areas. Therefore, VOIs for blood pool and fibrotic areas were drawn in selected slices, and diagrams with activity VOI content over acquisition time were derived.

The time-to-peak values (minutes from the beginning of the dynamic acquisition to the maximum of SUV_{max} of the lesion) were derived from the time-activity curves.

Statistical Analysis

TBR and SUV_{max} values of FDG PET/CT and ^{68}Ga-FAPI were analyzed descriptively reporting means and SDs. Moreover, the independent samples *t* test was applied to compare the ^{68}Ga-FAPI PET values of the pulmonary impaired patient group with the control group. Comparisons of ^{68}Ga-FAPI versus ^{18}F-FDG values were performed using paired samples *t* tests. Comparisons of ^{68}Ga-FAPI values within the pulmonary impaired patient group across the 3 different time points (30 minutes vs 60 minutes vs 120 minutes) were done using analysis of variance for repeated measurements and Bonferroni corrected post hoc tests.

All statistical tests were 2-sided at a significance level of 0.05. Statistical analyses were conducted in SPSS, version 26.0 (IBM Corp, Armonk, NY).

RESULTS

PET/CT imaging showed positive ^{68}Ga-FAPI uptake in all suspected fibrotic areas of post COVID-19 patients.

In static ^{68}Ga-FAPI imaging, the suspected pulmonary abnormalities in post COVID-19 patients showed for ^{68}Ga-FAPI a mean SUV_{max} of 3.81 ± 1.24 after 30 minutes, 2.75 ± 0.32 after 60 minutes, and 2.74 ± 0.31 after 120 minutes, respectively; the mean TBR was

1.65 ± 0.50 after 30 minutes, 2.05 ± 0.28 after 60 minutes, and 1.29 ± 0.32 after 120 minutes, respectively ($P_{\text{differences across all 3 time points}} = 0.279$); the mean TBR was 1.65 ± 0.50 after 30 minutes, 2.05 ± 0.28 after 60 minutes, and 1.29 ± 0.32 after 120 minutes, respectively ($P_{\text{differences across all 3 time points}} = 0.002$).

Specifically, we have found significantly higher TBR of ^{68}Ga-FAPI after 60 minutes in respect to TBR after 120 minutes ($P_{\text{Bonferroni correction}} = 0.009$).

The estimated mean SUV_{max} of ^{68}Ga-FAPI within the pulmonary parenchyma in the control group was 1.04 ± 0.25 and the TBR 0.74 ± 0.15, both after 60 minutes.

The ^{68}Ga-FAPI PET scans depicted significantly increased SUV_{max} and TBR values in the pulmonary impaired post COVID patient group compared with the control group (P values for both parameters <0.001).

In contrast to ^{68}Ga-FAPI, ^{18}F-FDG PET/CT imaging was visually negative on all patients. In relation to the glucose metabolical characterization of pulmonary lesions, the calculated SUV_{max} and TBR of ^{18}F-FDG PET were 2.05 ± 0.28 and 0.65 ± 0.12, respectively.

Furthermore, the ^{68}Ga-FAPI PET obtained after 60 minutes revealed significantly higher tracer uptake in term of SUV_{max} and TBR in residual fibrotic lesions in comparison to ^{18}F-FDG PET/CT ($P = 0.003$ and $P < 0.001$, respectively). A depictive case is shown in Figure 1.

The ^{68}Ga-FAPI time-activity curves for lung abnormalities showed an early peak just after median 40 seconds (range, 27–90 seconds postadministration) correlating with the aortic perfusion peak after 20 seconds (range, 13–90 seconds) and 25% clearance blood pool after 212 seconds (range, 139–333 seconds), followed by a slowly decreasing signal intensity in lung lesions over time.

At 6-month chest CT follow-up of post COVID-19 cohort, no improvement of lung abnormalities could be detected. The next chest CT follow-up was scheduled in 2 years.

DISCUSSION

Early lung function analysis of patients with COVID-19 at the time of discharge from hospital revealed a high rate of abnormalities indicative of potential interstitial lung disease.[17]

The load of fibrotic lung disease after SARS-CoV-2 infection is tending to be high; the global load of fibrotic lung disease will apparently increase remarkably.[18]

The early identification of patients at higher risk of lung injury and fibrotic damage is critical and therefore the necessity of diagnostic guidance for patients with persistent pulmonary abnormalities after COVID-19 infection appears to be eminent. The final origin of fibrotic findings in the lungs remains unknown: the viral infection, the secondary cytokine cascade, related to treatment or ventilation, or a mixture of all these factors come into consideration.[18]

The diagnosis of pulmonary fibrosis based on CT findings remains challenging: parenchymal bands, irregular interfaces, reticular opacities, and traction bronchiectasis with or without honeycombing not always clearly present on the follow-up CT scans.[19] Unfortunately, the histological confirmation appears also oft not executable or infeasible. Noninvasive clinical diagnostic performance is extremely advisable.

We intended to explore the potential diagnostic benefit of nuclear imaging in terms of PET/CT scanning in further characterization of impaired pulmonary convalescence.

Because the ^{18}F-FDG-PET/CT was negative and because no improvement on prolonged up to 3 months high-dose corticosteroids could be observed, we then assumed the presence of underlying fibrotic repair processes. This hypothesis is backed by former studies, which investigated the diagnostic yield of ^{68}Ga-FAPI PET/CT in lung cancer and IPF. The respective PET/CT analysis showed a low physiological background signal of FAP in tumor surrounding tissue, whereas increased tracer uptake in IPF-related fibrotic lesions was observed.[7,8,20] Furthermore, the calculated SUV_{max} of ^{68}Ga-FAPI within the fibrotic lesions was similar to the calculated SUV_{max} of the here presented post COVID-19 lesions.[21]

Within IgG4-related disease, ^{68}Ga-FAPI PET/CT was able to discriminate between inflammatory and fibrotic activity.[20]

Moreover, several trials (NCT04541680, NCT04619680, and NCT04607928) currently investigate the use of antifibrotic medication in COVID-19.

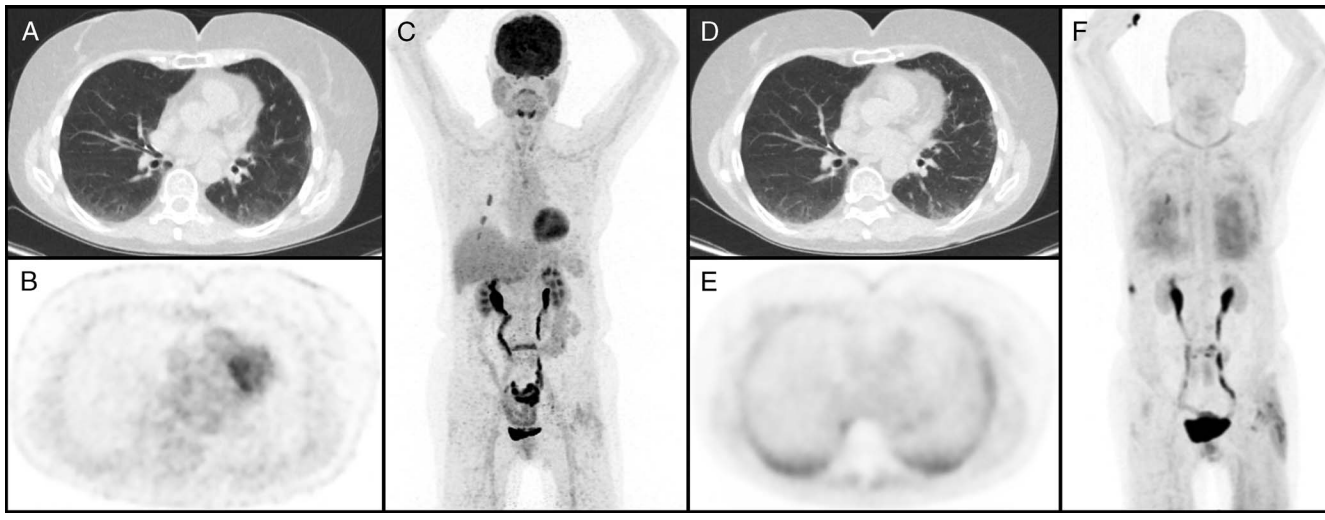

FIGURE 1. Comparison of ^{18}F-FDG PET/CT (**A**–**C**) and ^{68}Ga-FAPI-46 PET/CT (**D**–**F**): the corresponding transaxial low-dose CT scans (**A** and **D**) and PET emission scans (**B** and **E**), together with the coronal MIPs (**C** and **F**). Showing no relevant accumulation of FDG but an accumulation of FAPI-46, 19 weeks after discharge from hospital, in residual peripheral ground-glass opacities and subtle reticular changes shown in the corresponding low dose CT scans. In addition, a serial rib fractures rights and inflammatory changes in left hip were detected on both scans.

CONCLUSIONS

^{68}Ga-FAPI-46 PET/CT may enhance noninvasive clinical diagnostic performance in patients with long-term pulmonary CT abnormalities after severe SARS-CoV-2 infection by uncovering early fibrotic changes after severe respiratory infections such as COVID-19.

Although this study shows promising results, additional studies in larger populations are required to establish a general diagnostic guideline in patients with suspected post COVID pulmonary fibrosis.

ACKNOWLEDGMENTS

The authors gratefully acknowledge the radiopharmaceutical company SOFIE for the support and providing of FAPI precursor material and especially the Director of Clinical Development Dr Frank Valla Jr.

REFERENCES

1. Ng CK, Chan JW, Kwan TL, et al. Six month radiological and physiological outcomes in severe acute respiratory syndrome (SARS) survivors. *Thorax*. 2004;59:889–891.
2. Mo X, Jian W, Su Z, et al. Abnormal pulmonary function in COVID-19 patients at time of hospital discharge. *Eur Respir J*. 2020;55:2001217.
3. Pogatchnik BP, Swenson KE, Sharifi H, et al. Radiology-pathology correlation in recovered COVID-19, demonstrating organizing pneumonia. *Am J Respir Crit Care Med*. 2020;202:598–599.
4. Ajuria-Illarramendi O, Martinez-Lorca A, Orduña-Diez MDP. [^{18}F] FDG-PET/CT in different COVID-19 phases. *IDCases*. 2020;21:e00869.
5. Park JE, Lenter MC, Zimmermann RN, et al. Fibroblast activation protein, a dual specificity serine protease expressed in reactive human tumor stromal fibroblasts. *J Biol Chem*. 1999;274:36505–36512.
6. Loktev A, Lindner T, Burger EM, et al. Development of fibroblast activation protein-targeted radiotracers with improved tumor retention. *J Nucl Med*. 2019;60:1421–1429.
7. Siveke JT. Fibroblast-activating protein: targeting the roots of the tumor microenvironment. *J Nucl Med*. 2018;59:1412–1414.
8. Egger C, Cannet C, Gérard C, et al. Effects of the fibroblast activation protein inhibitor, PT100, in a murine model of pulmonary fibrosis. *Eur J Pharmacol*. 2017;809:64–72.
9. Varasteh Z, Mohanta S, Robu S, et al. Molecular imaging of fibroblast activity after myocardial infarction using a ^{68}Ga-labelled fibroblast activation protein inhibitor FAPI-04. *J Nucl Med*. 2019;60:1743–1749.
10. Kratochwil C, Flechsig P, Lindner T, et al. ^{68}Ga-FAPI PET/CT: tracer uptake in 28 different kinds of cancer. *J Nucl Med*. 2019;60:801–805.
11. Giesel FL, Heussel CP, Lindner T, et al. FAPI-PET/CT improves staging in a lung cancer patient with cerebral metastasis. *Eur J Nucl Med Mol Imaging*. 2019;46:1754–1755.
12. Chen H, Pang Y, Meng T, et al. ^{18}F-FDG and ^{68}Ga-FAPI PET/CT in the evaluation of ground-glass opacity nodule. *Clin Nucl Med*. 2021;46:424–426.
13. Zhao L, Pang Y, Sun L, et al. Increased ^{68}Ga-FAPI uptake in the pulmonary cryptococcus and the postradiotherapy inflammation. *Clin Nucl Med*. 2022; 47:243–245.
14. World Medical Association. World Medical Association Declaration of Helsinki: ethical principles for medical research involving human subjects. *JAMA*. 2013;310:2191–2194.
15. Spreckelmeyer S, Balzer M, Poetzsch S, et al. Fully-automated production of [^{68}Ga]Ga-FAPI-46 for clinical application. *EJNMMI Radiopharm Chem*. 2020;5:31.
16. Boellaard R, Delgado-Bolton R, Oyen WJ, et al. FDG PET/CT: EANM procedure guidelines for tumour imaging: version 2.0. *Eur J Nucl Med Mol Imaging*. 2015;42:328–354.
17. Rees EM, Nightingale ES, Jafari Y, et al. COVID-19 length of hospital stay: a systematic review and data synthesis. *BMC Med*. 2020;18:270.
18. George PM, Wells AU, Jenkins RG. Pulmonary fibrosis and COVID-19: the potential role for antifibrotic therapy. *Lancet Respir Med*. 2020;8:807–815.
19. Wang Y, Dong C, Hu Y, et al. Temporal changes of CT findings in 90 patients with COVID-19 pneumonia: a longitudinal study. *Radiology*. 2020; 296:E55–E64.
20. Schmidkonz C, Rauber S, Atzinger A, et al. Disentangling inflammatory from fibrotic disease activity by fibroblast activation protein imaging. *Ann Rheum Dis*. 2020;79:1485–1491.
21. Röhrich M, Leitz D, Flechsig P, et al. Fibroblast activation protein-specific PET/CT imaging in idiopathic pulmonary fibrosis with lung cancer. *J Nucl Med*. 2019;60(suppl 1):298.